EFFECT OF PUNCH STROKE APPLICATION STRATEGIES ON FORMING OF FUSELAGE PANEL LAY-UP MOLDS

MELİS HIZARCI

JUNE 2022

ÇANKAYA UNIVERSITY

GRADUATE SCHOOL OF NATURAL AND APPLIED SCIENCES

DEPARTMENT OF MECHANICAL ENGINEERING

MASTER THESIS IN

MECHANICAL ENGINEERING

EFFECT OF PUNCH STROKE APPLICATION STRATEGIES ON FORMING OF FUSELAGE PANEL LAY-UP MOLDS

MELİS HIZARCI

JUNE 2022

Title of the Thesis: **EFFECT OF PUNCH STROKE APPLICATION STRATEGIES ON FORMING OF FUSELAGE PANEL LAY-UP MOLDS**

Submitted by: **Melis Hızarcı**

Approval by the Graduate School of Natural and Applied Sciences, Çankaya University.

Prof. Dr. Ziya Esen
Director

I certify that this thesis satisfies all the requirements as a thesis for the degree of Choose

Prof. Dr. Haşmet Türkoğlu
Head of Department

This is to certify that I have read this thesis and that it is fully adequate in scope and quality as a thesis for the degree of Master of Science in Mechanical Engineering

Prof. Dr. Can Çoğun
Supervisor

Thesis Defense Date: 21.06.2022

Thesis Jury Members:

Prof. Dr. Can ÇOĞUN	Çankaya University	
Prof. Dr. Mustafa Yurdakul	Gazi University	
Assoc. Prof. Dr. Gökhan Küçüktürk	Gazi University	

STATEMENT OF NONPLAGIARISM

I hereby declare that all statements in this statement have been obtained and presented in accordance with academic rules and ethical conduct. I also declare that, as required by these rules and conduct, I have fully cited and referenced all material and results that are not original to this work.

Name, Last Name	**: Melis HIZARCI**
Signature	**:**
Date	**: 22/06/2022**

ABSTRACT

EFFECT OF PUNCH STROKE APPLICATION STRATEGIES ON FORMING OF FUSELAGE PANEL LAY-UP MOLDS

HIZARCI, Melis

Master of Science in Mechanical Engineering

Supervisor: Prof. Dr. Can ÇOĞUN

June 2022, 36 pages

This study proposed three punch stroke application strategies to cold form the Invar FeNi36 plate into a fuselage panel lay-up mold. The same number of punch strokes but at different positions was applied to the plate in the strategies. The strategies' effectiveness was evaluated using the Finite Element Method (FEM). The strategy yielded the closest form to the desired plate form was considered the best.

Keywords: Cold Forming, Forming strategy, Invar $FeNi_{36}$, Finite Element Analysis, QForm.

ÖZ

UÇAK GÖVDE PANEL YATIRMA KALIPLARININ ŞEKİLLENDİRİLMESİNDE ZIMBA VURUŞ STRATEJİLERİNİN ETKİSİ

HIZARCI, Melis

Master of Science in Mechanical Engineering

Danışman: Prof. Dr. Can ÇOĞUN

Haziran 2022, 36 sayfa

Bu çalışma, Invar FeNi36 plakasını gövde paneli yatırma kalıbına soğuk şekillendirmek için üç farklı zımba vuruş uygulama stratejisi önerilmiştir. Stratejilerde plakaya aynı sayıda ancak farklı pozisyonlarda zımba vuruşları uygulanmıştır. Stratejilerin etkinliği Sonlu Elemanlar Metodu (FEM) kullanılarak değerlendirilmiştir. İstenilen plaka formuna en yakın formu veren strateji en iyi olarak kabul edilmiştir.

Anahtar Kelimeler: Soğuk Şekillendirme, Şekillendirme Stratejisi, Invar $FeNi_{36}$, Sonlu Elemanlar Analizi, QForm

ACKNOWLEDGEMENT

I would like to express my sincere gratitude to my parents for their support and sacrifice to me. Your memories would ever shine in my mind.

Special thanks to my supervisor, Prof. Dr. Can ÇOĞUN for the excellent guidance and for providing me with an excellent atmosphere to conduct this research. I would like to thank Dr. Ferah SUCULARLI for his help in writing many parts of the thesis. My special gratitude also goes to the rest of the thesis committee Prof. Dr. Mustafa YURDAKUL, Doç. Dr. Gökhan KÜÇÜKTÜRK, for the encouragement and insightful comments

TABLE OF CONTENTS

LIST OF TABLES

LIST OF FIGURES

ABBREVIATIONS

CAD	:	Computer aided design
CNC	:	Computer numerical control
FEM		Finite Element Method
DOF	:	Degrees of freedom
FEA	:	Finite element Analysis

CHAPTER I

INTRODUCTION

Airplane fuselage panels being produced today are made of composite materials. The production of the necessary lay-up mold is one of the most critical stages of composite structure production and affects the product quality. The surface quality of the molds, the behavior of the mold materials at elevated temperatures (during firing, autoclave or curing) and the expansion-contraction properties directly affect the final product quality [1, 2]. In cases where many composite fuselage panels are desired, a durable lay-up mold will be necessary. Considering the cases where the mold is damaged or cannot be used again during the separation of the produced composite product, it should be perceived as an economic necessity to determine a mold production method according to the needs [1].

Molds are composed of Male Mold and Female Mold, whereas the male mold shapes the inner part of the structure and the female mold shapes the outer part of the structure [3]. Convex surfaces such as wings and fuselage are more common in aviation and space structures due to their aerodynamic properties, and therefore female molds are used more frequently. Since the outer surface quality is sought in the parts to be produced, either a one-to-one male model is produced and a female mold is obtained from this model, or the mold material is processed as a female mold in CNC and similar machines.

Although different methods are used for the composites to take the final shape, generally, the fibers in the form of fabric are laid-up on the mold (Figure 1.1). After the resin is injected, it enters the autoclave furnace for curing (Figure 1.2).

In producing the lay-up mold, the first stage is the cold forming of the plate material into the desired final form as close as possible. The second stage is machining the cold-formed plate to provide better lay-up surface roughness and dimensional accuracy. The cold-forming of lay-up mold reduces the machining time and cost. The machined mold is spot welded or fastened to the support structure

(fixture) (Figure 1.3) to constrain its movement during composite lay-up. Generally, the Invar (Nickel-Iron alloy) material is used as a lay-up mold in the production of the inner composite fuselage panels of the aircraft due to its low coefficient of expansion.

Figure 1.1: Composite Lay-Up

Figure 1.2: Autoclave Furnace

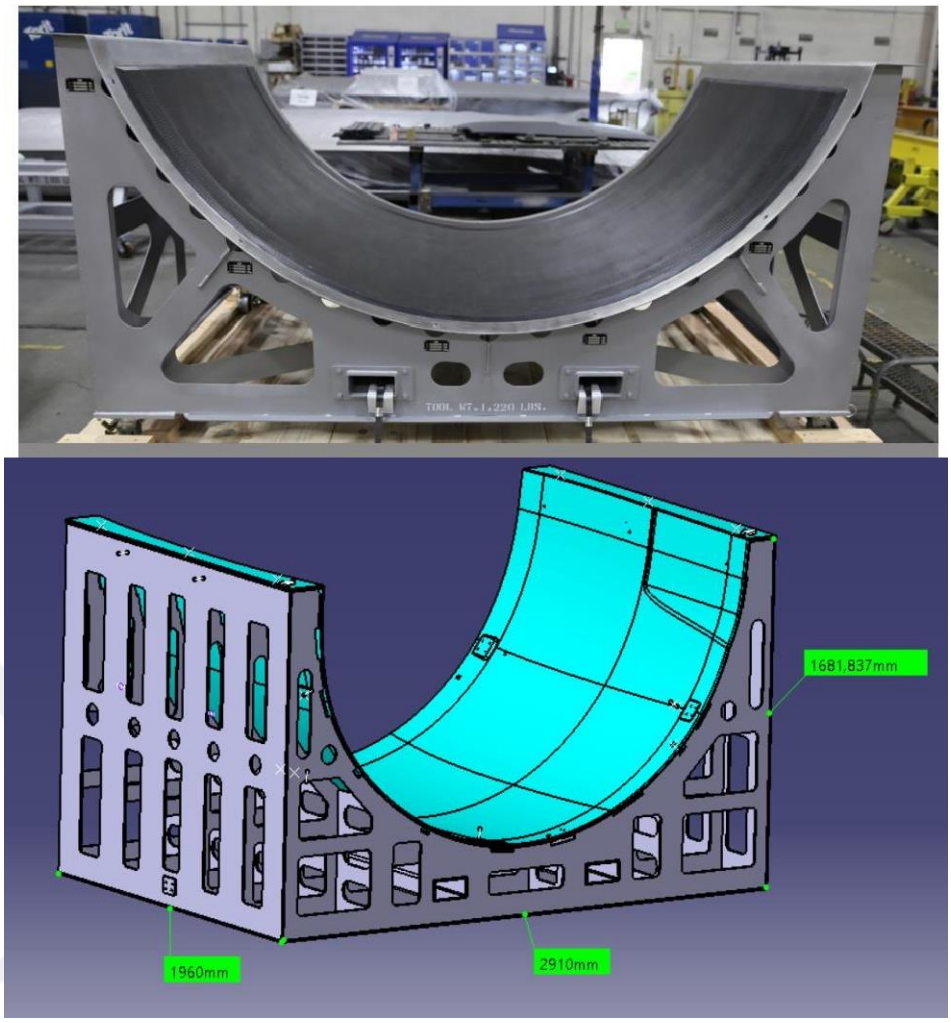

Figure 1.3: Lay-up Mold and Its Fixture

The production of the lay-up mold from a thick plate (about 1-inch thickness) by cold forming is the most critical step since it lowers the machining time and cost. A method called the "incremental sheet forming process" for cold forming the sheet material into irregular concave down form is introduced by Shahare et al. [9]. In this method, the die (hammer) slowly moves down the z-axis, following a linear path on the x- or y-axis. The hammer also simultaneously applies strokes (hammerings) to the plate to form incrementally. Since the technique is only valid for thin sheets (about 1 mm), it is not applicable for the cold forming of thick plates (above 1-inch thickness), which is the primary concern of this thesis. In another research on spring-back of the three-dimensionally curved metal plates shaped by cold forming plate, multiple small punches were combined to form the male and female molds. The forming method is named as "multi-point forming proses". The results revealed that the spring back increased and forming the plate became difficult when plate

thickness was increased [10]. In Li and Hu's study [11], ultrasonic vibration is applied to enhance the cold forming of sheet material in the multi-point forming proses. The finite element analysis results revealed that forming the sheet with vibration enhanced the forming accuracy (less spring back) compared with the no-vibration cases. In Bojahr et al. study [12], a 1-inch thick plate was formed by combining rolling and bending processes using multiple rolls. Since the produced forms are continuous, the plates' final form was not exactly in 3-D curvatures.

In nowadays level of technology, the application points of the punch strokes on the plate surface during cold-forming operation depend on the previous experience of the press operator. The operator does not know precisely the effect of punch application points on the final geometry of the plate. So, there is a strong need for research studies on the effect of punch application points on the final shape of the cold-formed plate. In this study, three punch stroke application strategies were proposed to cold form the Invar FeNi36 plate into a fuselage panel mold to fill the literature gap. The same number of punch strokes but at different positions was applied to the plate in the strategies. The strategies' effectiveness was evaluated using the Finite Element Method (FEM). The strategy that yielded the closest form to the desired plate form was considered the best strategy among the others.

CHAPTER II
THE COLD FORMING OF LAY-UP MOLD

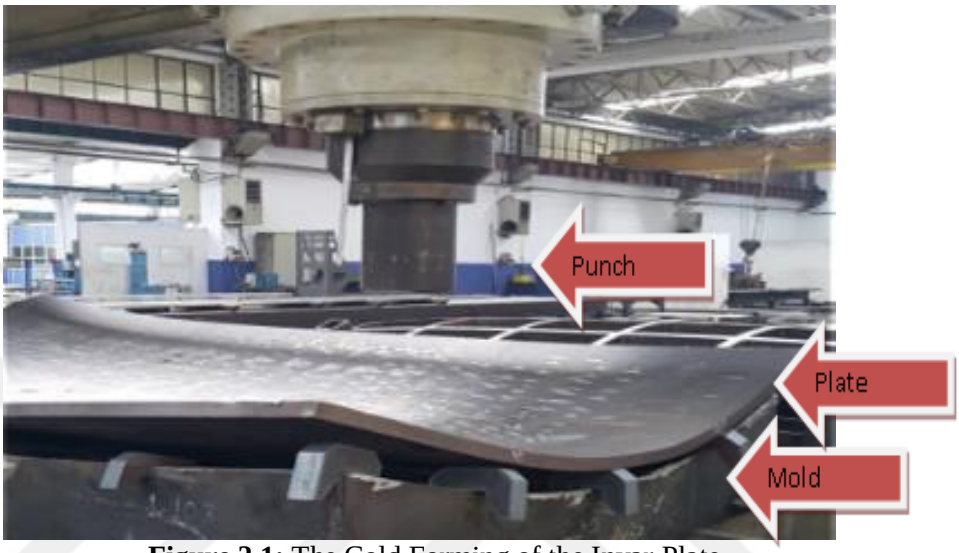

Figure 2.1: The Cold Forming of the Invar Plate

As shown in Figure 2.1, the punch strokes the plate to fit it into the shape of the bottom female mold. Vertical plates support the mold. The mentioned technique is applied in the cold-forming of thick Invar plates (about 25 mm thick) only in a limited number of companies in Türkiye.

Figure 2.2: The Plate After Cold-Forming

At the end of each punch stroke, a slight plastic deformation (penetration) on the plate surface is also observed (Figure 2.2). When the punch is retracted, a spring-back occurs. The fewer punch strokes will yield less damage on the plate and extend female mold life. The correct positions and sequences of punch strokes with a minimum number will result in a faster and geometrically reliable (i.e., the desired final form) cold forming operation.

In this study, before the application of punch strokes, the plate was deep-drawn by a male mold (Figure 2.3) to reduce the number of punch strokes and yield a much closer plate form to the desired.

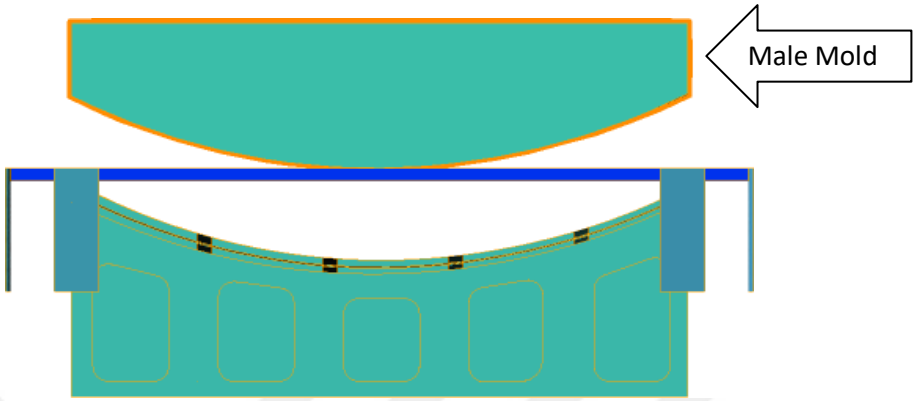

Figure 2.3: Plate Material, Male and Female Molds

CHAPTER III

MATERIAL AND METHOD

1.1 FINITE ELEMENT METHOD (FEM)

In this study, the cold forming of the fuselage panel lay-up mold is simulated by FEM using the QForm 10 Metal Forming Simulation software (shortly, QFform). In this part of the thesis, the material properties, boundary conditions and motion constraints of the mold, punch and invar plate are given.

1.1.1 QForm Simulation Program

QForm is used for cold forging, hot forging, rolling, aluminum profile extrusion and other metal forming processes. It has been designed to conduct optimization studies in the program microstructure, thermal process analysis, and user-specified custom substructure. There are modules with various additional features, such as creating functions and simulation of die stress-strain state for cold forming [4]. The software is compatible with automatic mesh generation infrastructure [5]. Automatic re-meshing is done without user intervention during analysis. It is necessary to input the process type (with or without regard to the heat problem), problem type (2D or 3D deformation), workpiece and tool geometry, workpiece parameters, including the parameters of the material rheological model, initial temperature and accumulated degree of deformation, tool parameters, including tool material rheological model, lubricant properties, type and parameters of equipment actuating the tool, boundary conditions, conditions of operation completion etc. [6]. Since the deformation problem is nonlinear, it is resolved with the iterative method. The user can choose an explicit or implicit multi-step procedure organization method. The difference between the explicit and implicit methods is determining the location of finite element mesh nodes at the simulation step.

1.1.2 Modeling

The analyzed system consists of four parts: A female mold (Figure 3.1), eight limiting plates (Figure 3.2), a 25 mm thick Invar plate (Figure 3.3) and a punch (Figure 3.4). Except for the Invar plate, the others were considered rigid in the analysis. The overall system is given in Figure 3.5. In this study, the initial forming of the plate by the deep drawing process (Figure 2.3) was not included in the FE analysis. Initially, the plate was assumed to contact the female mold at the outer ends (670 mm in length). The maximum distance between the plate and the female mold at the plate's center was assumed to be 25 mm.

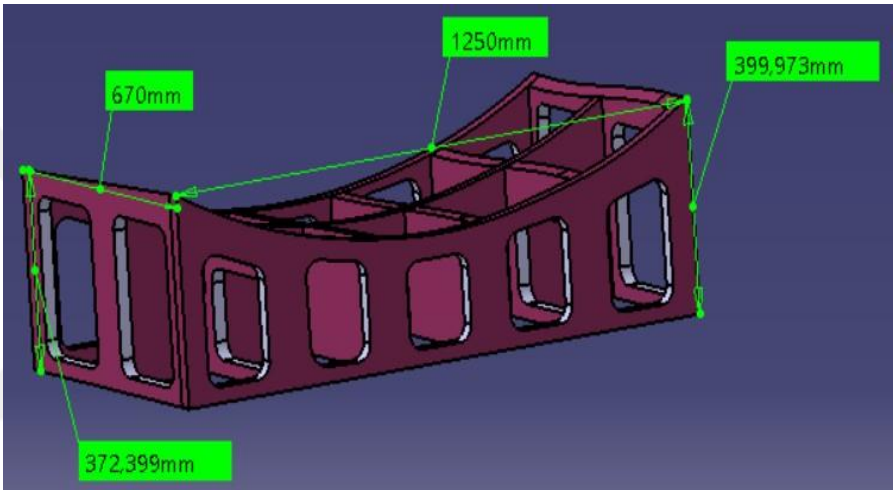

Figure 3.1: Female Mold

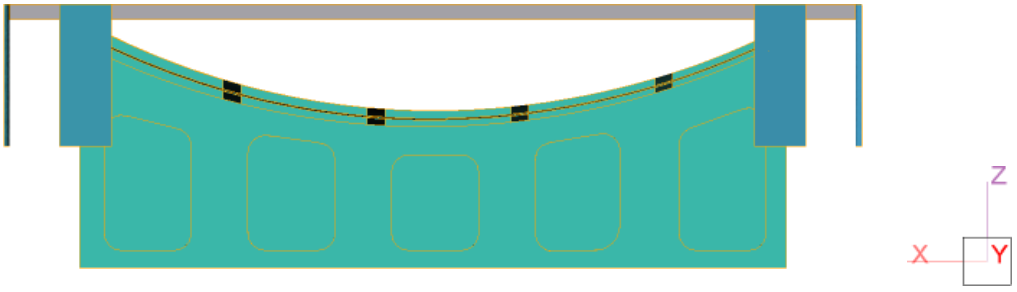

Figure 3.2: Eight Limiting Plates

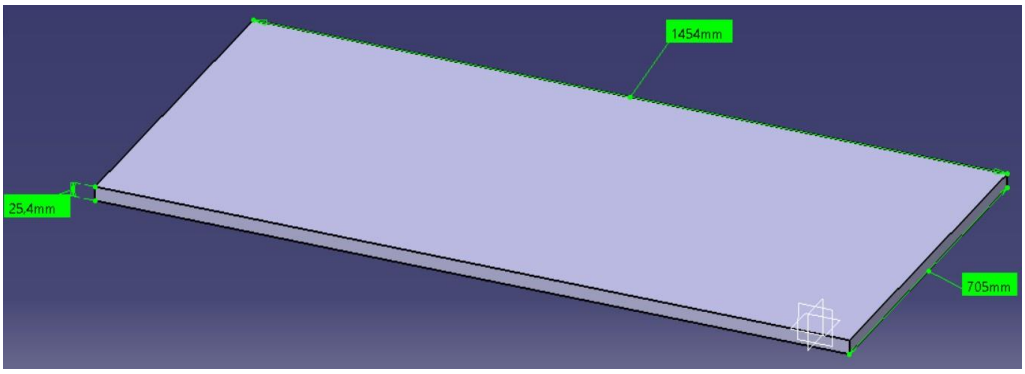

Figure 3.3: Invar Plate

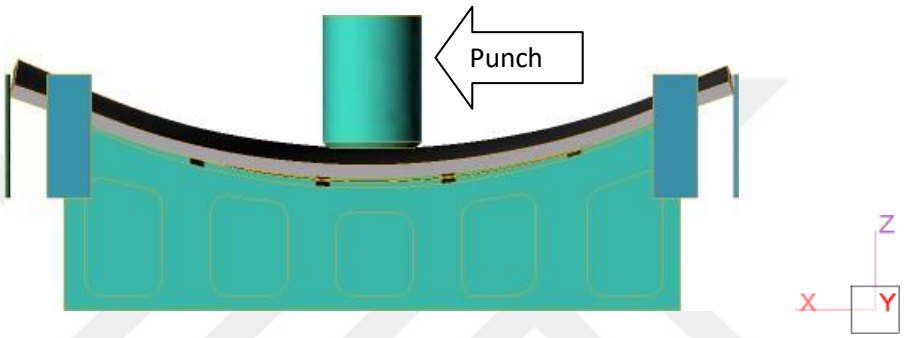

Figure 3.4: Punch

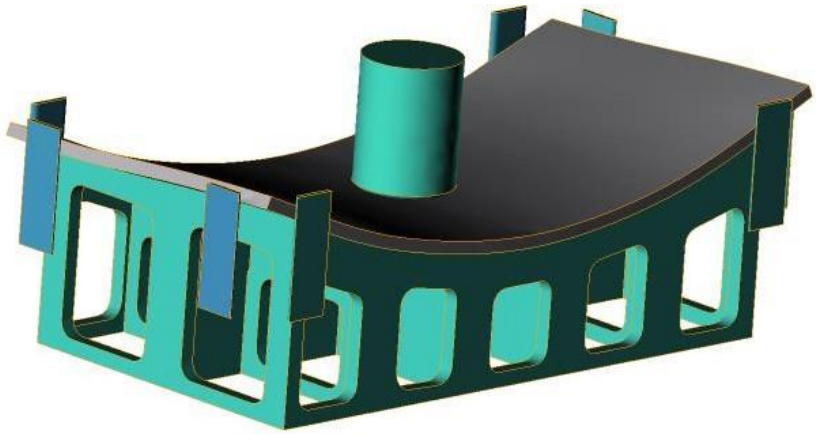

Figure 3.5: Assembly of the System

1.1.3 Plate Material

The plate material is Invar (Nilo Alloy 36, 36% Ni and 64% Fe, UNS K93600 and UNS K93601 [7]). Due to its low expansion coefficient, it is frequently used in aviation, composite materials, reference lengths, measuring devices and meters and parts requiring high precision. The material strength properties (Table 3.1) are found

by tensile testing of five specimens from the same Invar plate. The stress vs. strain characteristics is given in Figure 3.7.

Table 3.3: Tensile test results of the Invar material (for five specimens)

Tensile stress at yield (at offset 0.2%), MPa	276-280
UTS, MPa	425-427
Tensile strain, %	31-32
Break-tensile stress, MPa	275-278
Break-tensile strain, %	44-44,5
Young's Modulus, MPa	140800-141800
Energy at break, J	340-345

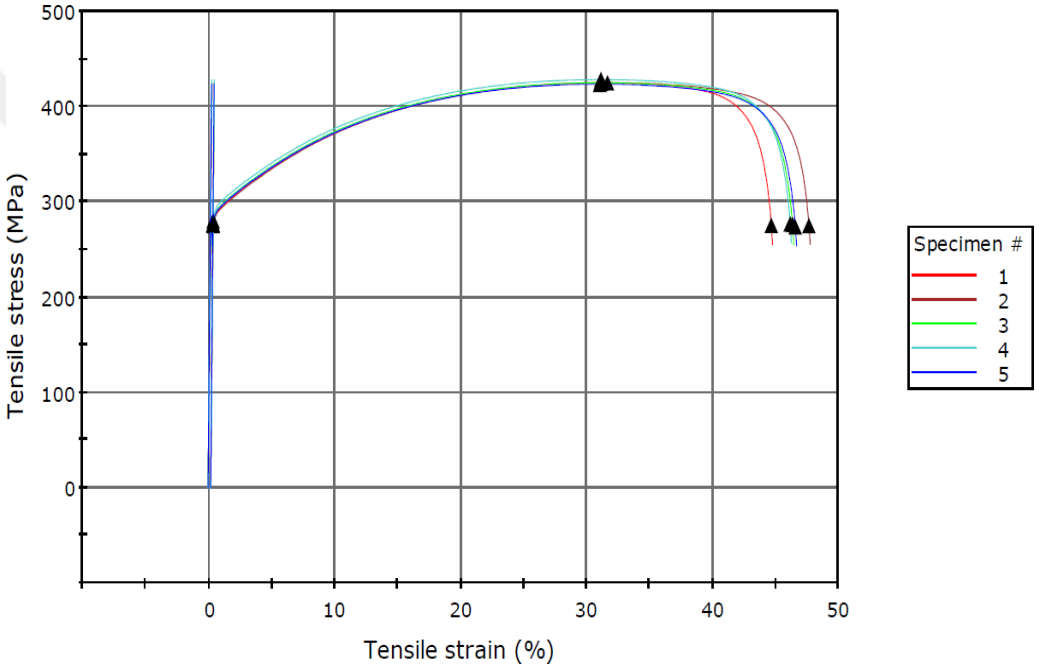

Figure 3.6: Tensile stress vs. Strain Plot for Specimens 1-5

1.1.4 Boundary Conditions and motions

The female mold movements in the x, y and z axes are constrained. Eight plates are welded to the plate to constrain its movements in the x and y axes (Figures 3.2 and 3.5). The plate elements' rotational and x, y and z linear motions are free. Although the male mold shown in Figure 2.3 is used to give the plate initial form by deep drawing, its FEM and FE analysis was not included in this study. The male mold is allowed to move in the z-direction. The punch can move in the x, y, and z axes. After contacting the plate, the punch can move a 25 mm maximum in the -z-direction (Figure 3.8). If the distance between the punch and the mold was less than

25 mm at the instant of the punch and the plate contact, then the punch –z motion was stopped when the plate contacted the female mold.

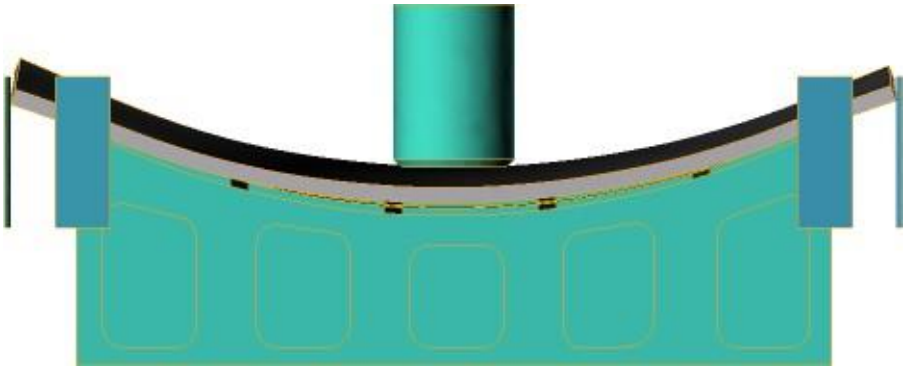

Figure 3.7: Maximum punch movement distance at the center of the plate (about 25 mm)

A hydraulic press was used in the analysis. The punch's maximum force and speed were defined as 10 MN and 25 mm/s. The analysis program worked with the displacement principle. When the punch descends a maximum of 25 mm after the punch-plate contact, the plate is assumed to touch the female mold and then punch retracts.

1.1.5 Meshing

The mesh geometry used in the analysis is tetrahedral. The re-meshing was done automatically by the software (Figure 3.9). In Table 3.2, the number of nodes and elements before and after the plate contacts the female mold is given.

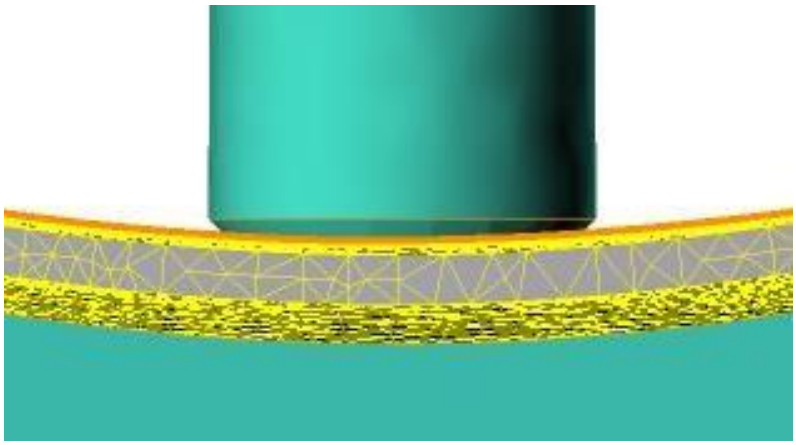

(a)

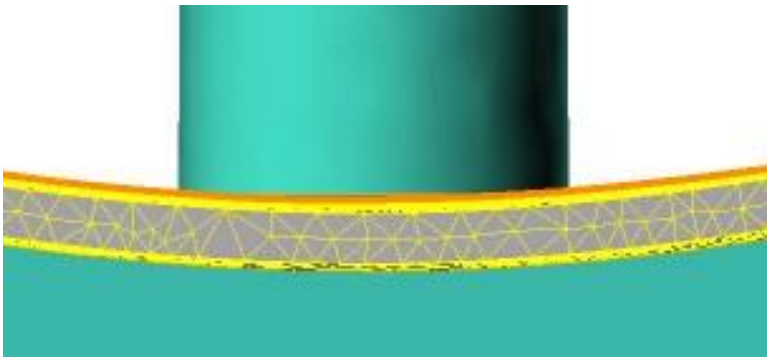

(b)

Figure 3.8: Mesh Structures and Re-meshing. a) Before and b) After the Invar Plate Contacts the Female Mold

Table 3. 4: Number of Nodes and Elements Before and After the Plate Contacts the Mold (Operation 1)

	Before Remeshing	After Remeshing
Nodes (on the surface)	7528	8810
Elements (on the surface)	15052	17616
Total Nodes of the plate	8808	10946
Total elements of the plate	30950	40101

1.1.6 Punch Stroke Application Strategies

In this study, three punch stroke application strategies (S1, S2 and S3) were proposed to cold form the Invar FeNi36 plate into a fuselage panel mold. The same number of punch strokes but at different positions was applied in the strategies. The strategies are designed according to the experience of the press operators and general rules of cold forming. The best strategy is the one that completes the forming operation with minimum deviation from the plate's desired (ideal) shape. In this study, the ideal plate shape is the shape of the female mold. The deviation of the cold-formed plate from the ideal was found by calculating the volume between them. The volumetric calculations were done according to the results obtained from the QForm analysis. The space between the final shape of the plate and the ideal form was converted into a solid model (Figure 3.10). Afterward, the volume of the solid model was calculated. The strategy with minimum volume indicated the best strategy.

The punch stroke sequences, x, y coordinates and the plate's forms in some instances of S1-S3 strategies are shown in Figures 3.11-3.13. The horizontal distance

between the successive punch strokes was chosen for all strategies as 150 mm. This distance enabled covering the overall plate surface in 35 punch strokes.

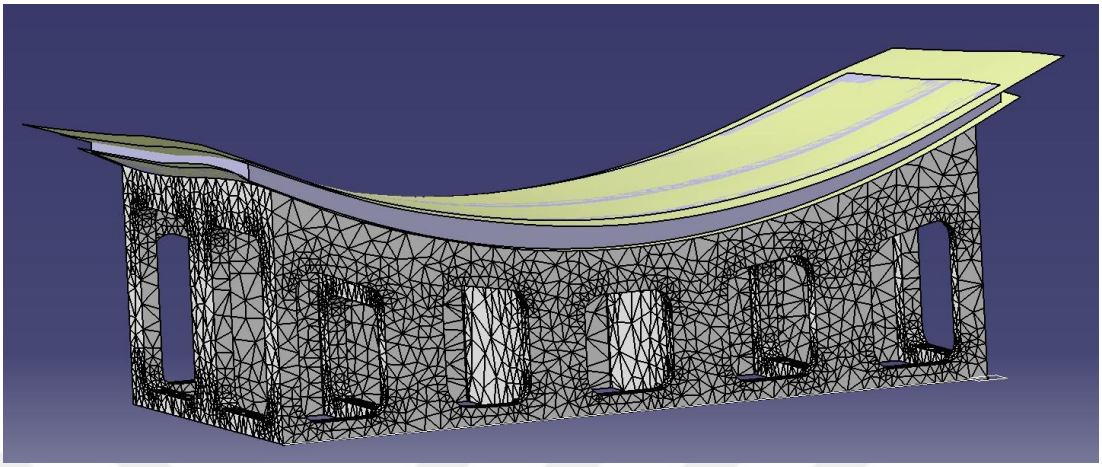

Figure 3.9: The solid model created between the female mold and cold-formed plate.

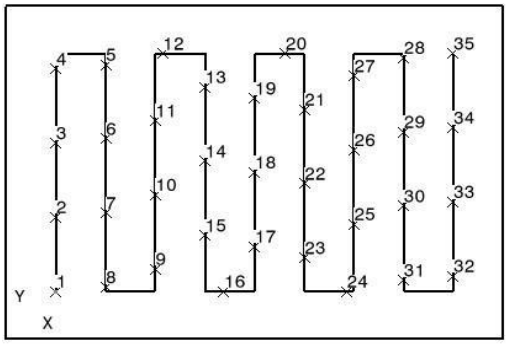

REF.	X	Y
1	0	0
2	0	15,59
3	0	31,18
4	0	46,76
5	10	47,65
6	10	32,06
7	10	16,47
8	10	0,88
9	20	4,71
10	20	20,29
11	20	35,88
12	21,47	50
13	30	42,94
14	30	27,35
15	30	11,76
16	33,82	0
17	40	9,41
18	40	25
19	40	40,59
20	46,18	50
21	50	38,24
22	50	22,65
23	50	7,06
24	58,53	0
25	60	14,12
26	60	29,71
27	60	45,29
28	70	49,12
29	70	33,53
30	70	17,94
31	70	2,35
32	80	3,24
33	80	18,82
34	80	34,41
35	80	50

(a)

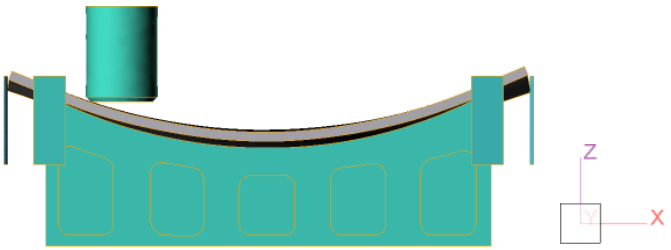

(b)

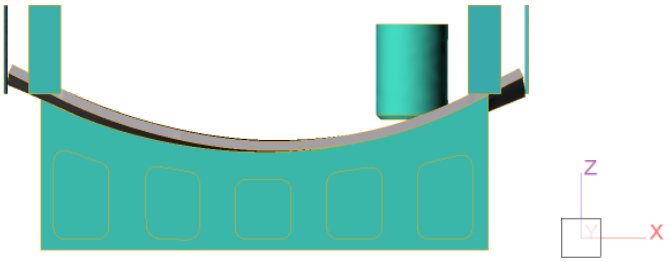

(c)

Figure 3.10: S1. a) Coordinates and sequence of punch strokes, b) plate geometry at the end of the first punch stroke, c) plate geometry at the end of the 35th punch stroke (coordinates in cm).

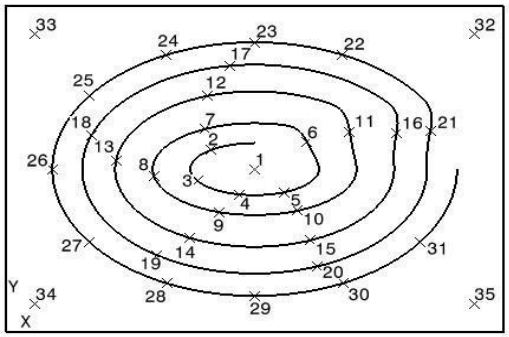

REF.	X	Y
1	0	0
2	-8,88	4,06
3	-11,49	-2,56
4	-3,02	-5,44
5	6	-4,96
6	10,5	5,82
7	-10,02	8,61
8	-20,23	-1,45
9	-7,15	-9,25
10	8,64	-8,95
11	19,07	8,06
12	-9,36	15,75
13	-27,82	1,83
14	-12,93	-14,82
15	11,16	-15,33
16	28,47	7,77
17	-4,96	22,24
18	-32,73	7,29
19	-19,64	-18,5
20	12,45	-20,96
21	35,23	8,25
22	17,61	24,58
23	-0,04	27,29
24	-17,7	24,56
25	-33,15	15,74
26	-40,58	-0,03
27	-33,11	-15,78
28	-17,64	-24,57
29	0,01	-27,29
30	17,67	-24,57
31	33,13	-15,76
32	44	29
33	-44	29
34	-44	-29
35	44	-29

(a)

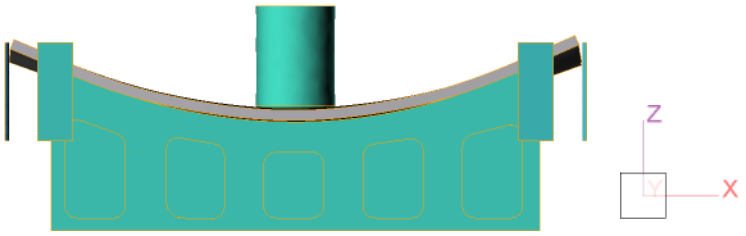

(b)

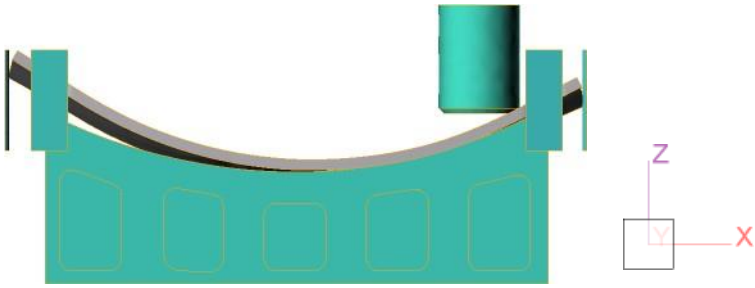

(c)

Figure 3.11: S2. a) Coordinates and sequence of punch strokes, b) plate geometry at the end of the first punch stroke, c) plate geometry at the end of the 35th punch stroke.

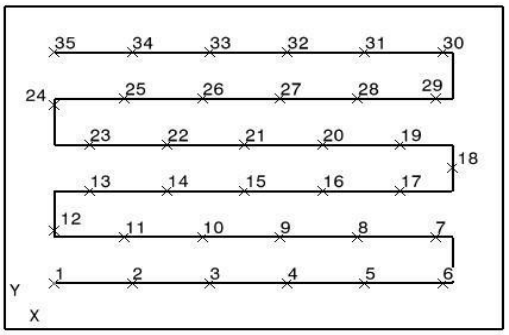

REF.	X	Y
1	0	0
2	15,59	0
3	31,18	0
4	46,76	0
5	62,35	0
6	77,94	0
7	76,47	10
8	60,88	10
9	45,29	10
10	29,71	10
11	14,12	10
12	0	11,47
13	7,06	20
14	22,65	20
15	38,24	20
16	53,82	20
17	69,41	20
18	80	25
19	69,41	30
20	53,82	30
21	38,24	30
22	22,65	30
23	7,06	30
24	0	38,53
25	14,12	40
26	29,71	40
27	45,29	40
28	60,88	40
29	76,47	40
30	77,94	50
31	62,35	50
32	46,76	50
33	31,18	50
34	15,59	50
35	0	50

(a)

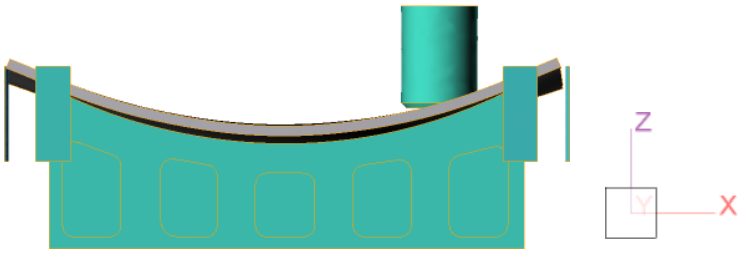

(b)

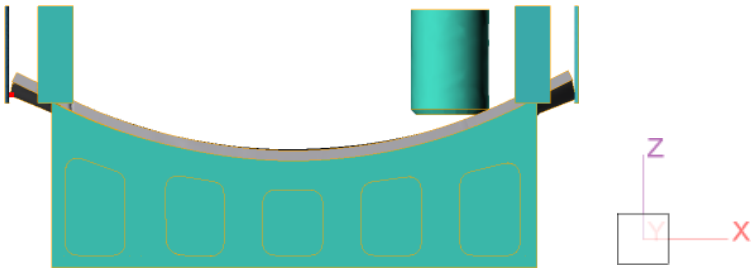

(c)

Figure 3.12: S3. a) Coordinates and sequence of punch strokes, b) plate geometry at the end of the first punch stroke, c) plate geometry at the end of the 35th punch stroke.

CHAPTER IV

RESULTS AND DISCUSSION

The following results are obtained at the end of the FEM and simulation of the processes:

1) A maximum of 25 mm distance was observed between the mid-bottom surface of the plate and the mold after the deep drawing of the plate by the male mold (Figure 2.3) due to spring back.
2) The volumes of the solid models created between the cold-formed plate and the ideal plate form in the S1 and S2 were higher than that of S3 (Table 4.1). The S1 and S2 yielded 216% and 333% higher volumes than the S3. In this study, a mean distance between the final shape and the ideal plate form was also defined. The distance was found by dividing the calculated volume by the area of the plate (1.25 x 0.67=0.838 m^2). Although the mean distance was not equally distributed on the surface, it provided a metric for comparing distances between ideal and actual plate forms for the strategies. As shown in Table 4.1, the mean distance was the lowest in S3 and the highest in S2. This result is consistent with the volumetric differences found for the strategies. So, it was deduced that the S3 was the best strategy among the others in reaching the ideal plate form, whereas S2 was the worst.
3) In this study, the plate's maximum temperature (T_{max}) under the punch at the instant of contact with the mold was also investigated. The plate's temperature rise under the punch was due to the plastic deformation of the plate in bending and squeezing modes. Figure 4.1 indicated that the T_{max} range, except for a few stroke positions, was 22-50^oC. At the first 15 strokes, the S2 yielded higher temperatures than the other strategies. The equivalent plastic strain (ε_{ep}) values at the instant plate contact with the mold were also found by FE analysis for each stroke of the strategies (Figure 4.2). The ε_{ep} increment $d\varepsilon_p$ was calculated from,

$$\bar{d}\epsilon_P = \sqrt{\frac{2}{3}\sum_{i=1}^{3}\sum_{j=1}^{3} d\epsilon_i^{(p)}\, d\epsilon_j^{(p)}} \geq 0.$$

Here, $d\varepsilon_{ij}^{(p)}$ is the equivalent strain increment component in the principal direction. The ε_{ep} values observed in the strategies were between 0.0065 and 0.016. Since the plastic deformation (yield) was assumed to start at 0.002 strain (0.2% offset), the ε_{ep} values of the strategies were high enough to cause plastic deformation of the plate. So, the temperature rise was attributed mainly to the plastic squeezing of the Invar material with the punch down movement (i.e., stroke). The local plastic deformation (penetration) marks on the plate surface (Figure 2.1) due to the localized high compressive stress exerted by the sharp punch side explains the slight temperature rise (typically 10 to 25 ^{o}C) on the plate.

The ε_{ep} values were very close for S1 and S3. Yet, S2 yielded much higher ε_{ep} values than the other two. The higher ε_{ep} values observed in S2 (Figure 4.2) resulted in the higher maximum temperatures (Figure 4.1).

4) In this study, maximum stress (Von Misses based, σ_{max}) values of the plate under the punch at the instant of contact with the mold were also studied. The variations of σ_{max} with punch stroke sequence for the S1-S3 are shown in Figure 4.3. The σ_{max} values, between 260-500 MPa, were generally higher than the yield strength of the Invar material (276-280 MPa) in all strategies causing the plastic deformation of the plate locally (i.e., penetration marks).

Table 4.1: The volume difference and mean distance between the final shape of the cold-formed plate and the ideal form for the strategies

Strategy	Volume difference (m^3)	Mean distance (m)
S1	0.026	0.031
S2	0.040	0.048
S3	0.012	0.014

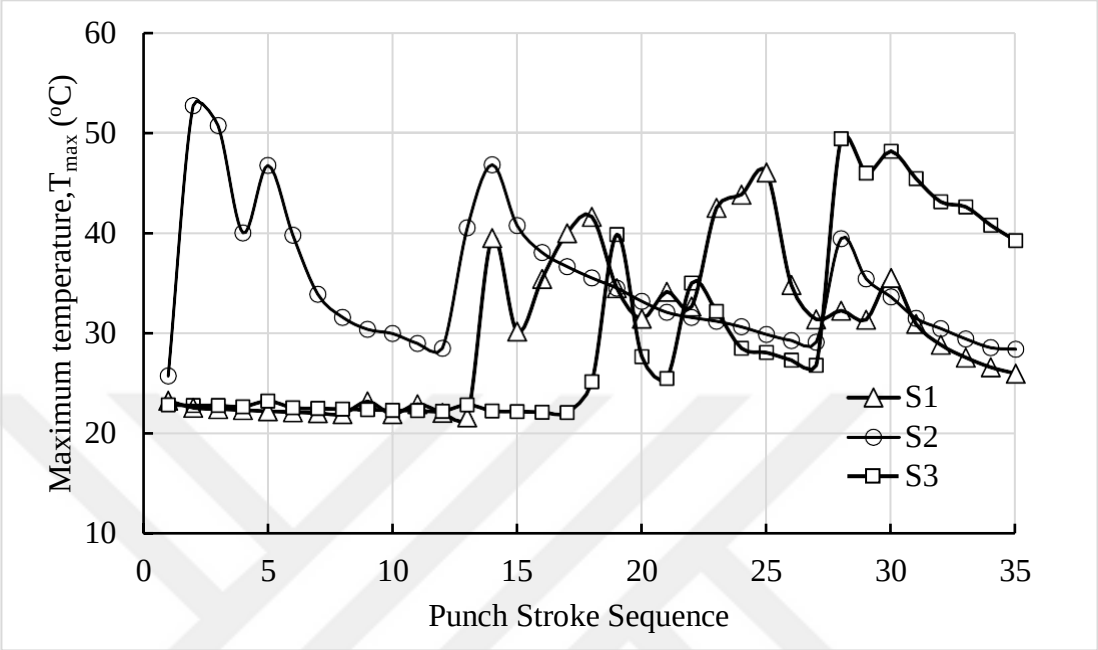

Figure 4.1: Variation of T_{max} with Punch Stroke Sequence for the S1-S3

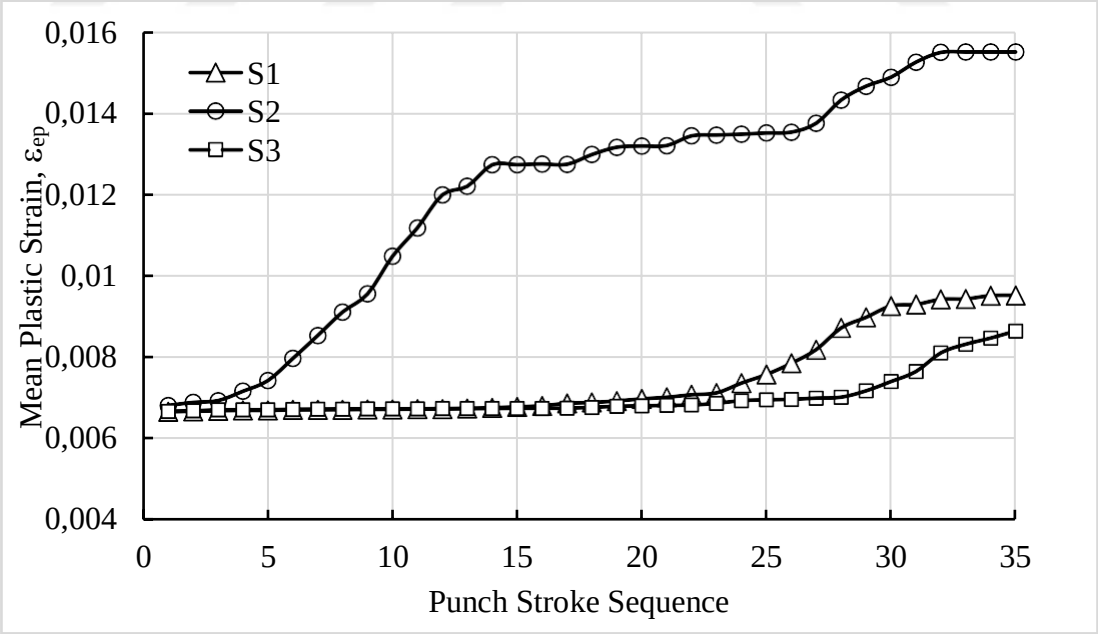

Figure 4.2: Variation of ε_{ep} with Punch Stroke Sequence for the S1-S3

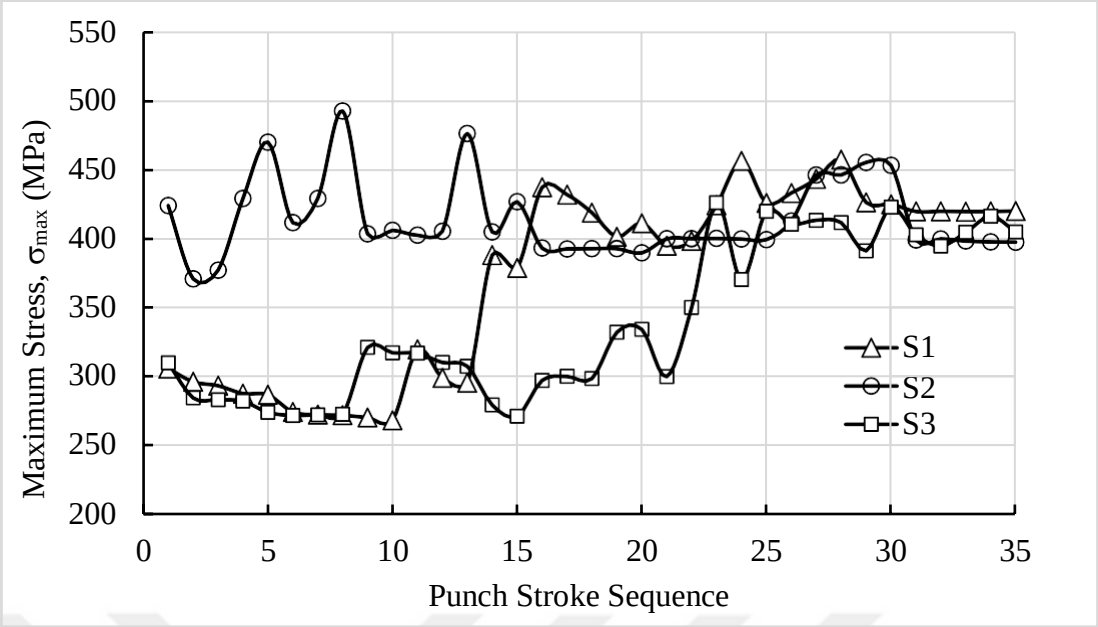

Figure 4.3: Variation of σ_{max} with Punch Stroke Sequence for the S1-S3

CHAPTER V

CONCLUSION

This study proposed three punch stroke application strategies (S1-S3) to cold form the Invar FeNi36 plate into a fuselage panel lay-up mold. The strategies' effectiveness was evaluated using the Finite Element Method (FEM). The following conclusions are drawn from the FEM and simulation of the processes:

-The S3 was the best strategy among the others in reaching the ideal plate form, whereas S2 was the worst.

-The equivalent plastic strain (ε_{ep}) values at the instant plate contact with the mold were high enough to cause plastic deformation of the Invar plate. So, the temperature rise was attributed mainly to the plastic squeezing of the plate with the punch stroke. The higher ε_{ep} values observed in S2 resulted in higher maximum temperatures.

-The maximum stress (σ_{max}) values of the plate under the punch at the instant of contact with the mold were higher than the yield strength of the Invar material (276-280 MPa) in all strategies causing the plastic deformation (penetration marks) of the plate locally.

REFERENCES

[1] DEMİRCAN Alpay, KAYRAN Altan ve KURTULUŞ D. Funda (2012), "Kompozit Yapılı Mini İHA'lar İçin Kalıp Üretim Teknikleri ve Aerodinamik Yüzeylerin Üretimi", IV. Ulusal Havacılık ve Uzay Konferansı, ss. 1-13, Hava Harp Okulu, İstanbul.

[2] TÖRE Cahit (2020), "Uçakların Yapısal Üretim Teknikleri ve İmalat Takımları (Takım=T00l, Aparat) (Konserve veya Kola Kutusundan Uçak Gövdesi İmalatı Yapılabilir mi?)", *Mühendis ve Makine*, Cilt 43, Sayı 506, ss. 33-38.

[3] Milli Eğitim Bakanlığı (2008), *Makina Enjeksiyon Kalıpçılığı 2*, MEGEP, Ankara.

[4] QForm (t.y.), *Cold Forming*. https://qform3d.com/processes/cold, ET. 12.01.2022.

[5] QForm (t.y.), *Software for Simulation and Optimization of Metal Forming Processes and Metal Profile Extrusion*. https://www.qform3d.com/products/qform, ET. 15.01.2022.

[6] QForm (t.y.), *10.1-Manual*. https://qform3d.com, ET. 20.02.2022.

[7] Hastelloy, C. (2020), *Invar 36*. https://www.defencemetal.com/invar-36/), ET. 20.02.2022

[8] KÖKEN Ali ve KURT Ertuğrul (2022), *Nonlinear Finite Elements Analysis of Different Steel Connections Using Ansys Workbench*, Konya Teknik Üniversitesi.

[9] Shahare, H. Y., Dubey, A. K., Kumar, P., Yu, H., Pesin, A., Pustovoytov, D., & Tandon, P. (2021). A Comparative Investigation of Conventional and Hammering-Assisted Incremental Sheet Forming Processes for AA1050 H14 Sheets. Metals, 11(11), 1862.

[10] Paik, J. K., Kim, J. H., Kim, B. J., & Tak, C. H. (2010,). Analysis of spring-back behavior in the cold-forming process of three-dimensionally curved metal plates. International Conference on Offshore Mechanics and Arctic Engineering (Vol. 49101, pp. 929-934).

[11] Li, X., & Hu, S. (2021). Research Progress of Springback in Multi-Point Forming of Sheet Metal. In Journal of Physics: Conference Series (Vol. 2101, No. 1, p. 012006). IOP Publishing.

[12] Bojahr, M., Prommer, H., Tschullik, R., & Kaeding, P. (2011). 3-Dimensional Forming of Thick Plates–A Comparison of Deep Drawing and an Approach of Rolling and Bending within a Single Process. In LSDYNA-Conference, Strasbourg